

Paper-Based Flexible Nanoparticle Hybrid Substrate for Qualitative and Quantitative Analysis of Melamine in Powder Milk by SERS

Published as part of ACS Omega virtual special issue "Celebrating 50 Years of Surface Enhanced Spectroscopy".

Akanksha Yadav, Anil K. Yadav,* Nazia Tarannum, and Dev Kumar



Cite This: *ACS Omega* 2024, 9, 2687–2695



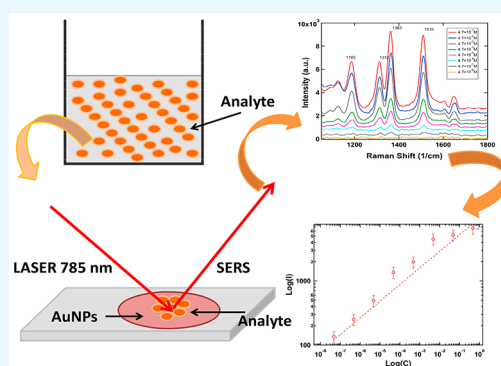
Read Online

ACCESS |

Metrics & More

Article Recommendations

ABSTRACT: Melamine is a chemical compound that is added to dairy products to increase the apparent protein content for higher profit margins. However, extended consumption of melamine can cause health risks. The SERS technique has proven to be an important tool for detecting small compounds, such as melamine. Here, a paper-based flexible nanoparticles (NPs)-hybrid SERS substrate was designed by drop-casting pegylated gold nanoparticles (AuNPs) on the filter papers. In SERS characterization, this substrate exhibited an enhancement factor of 10^8 and a limit of detection (LOD) as low as 10^{-8} M for Rhodamine 6G dye. Furthermore, we successfully utilized these substrates to detect the melamine spiked milk sample with an LOD as low as 0.01 ppm. This hybrid SERS substrate offers a low-cost, biocompatible, and easy-to-use fabrication for large-scale production, which may be widely used in food safety applications.



1. INTRODUCTION

The discovery of surface-enhanced Raman scattering (SERS) in the mid-1970s by Fleischmann and colleagues¹ has wide-range use. Since its discovery, SERS has been employed for the detection of a vestige of analytes owing to its reliable, adaptable, and label-free method of gaining information on molecular fingerprint(s).² The two primary mechanisms for Raman enhancements are (i) electromagnetic enhancement, which is linked to the local surface plasmon resonance on the nearby noble metal nanostructures, and (ii) the chemical enhancement caused by the charge transfer.³ Due to its reliable performance, SERS can be used as a detection tool in various applications including forensics, bio-sensing, environmental pollution, and detection of contamination in food products.

The aspirations of a healthy and disease-free life are often challenged by poor food quality. The edible items present in the kitchen are regularly contaminated with additives.⁴ According to a 2018–2019 report released by the Food Safety and Standards Authority of India (FSSAI), ~28% of the food samples are contaminated or of inferior quality.⁵ If people or animals consume such tainted food for an extended period, they will encounter deteriorated health.

Melamine ($C_3H_6N_6$) is an organic compound commonly used as an additive in dairy products. It is a rich source of nitrogen, mimicking a rich nitrogen content similar to that in natural proteins. It is purposefully added to low-quality milk or in other dairy products to increase apparent protein content detected by the Kjeldahl and Dumas test.⁶ Of note, the

Kjeldahl and Dumas test is a widely used method for determining the protein content of foods.⁷ The World Health Organization (WHO) recommended melamine content is 1 mg L^{-1} for infant formula and 2.5 mg L^{-1} for milk and food products. When melamine is consumed for an extended period above the WHO recommended limits, cyanuric acid (a well-known kidney toxicant) reacts with it and creates yellow crystals that can block kidney functions, which can be fatal.⁸ The “milk crisis” of 2008, which occurred in China caused the death of 6 infants due to the consumption of melamine-containing infant milk with ~860 hospitalizations.⁹ For this reason, it is therefore vital to monitor the melamine content present in food items, particularly in milk and infant formula. Traditional methods, such as gas chromatography (GC), liquid chromatography (LC), high-performance liquid chromatography (HPLC), or mass spectrometry (MS), are very sensitive and accurate detection methods.^{10,11} However, they are time-consuming, require skilled manpower, and are expensive.⁷ While these techniques are affordable in resource-rich settings, these techniques are not frequently available in low- and

Received: October 3, 2023

Revised: November 12, 2023

Accepted: December 7, 2023

Published: January 5, 2024



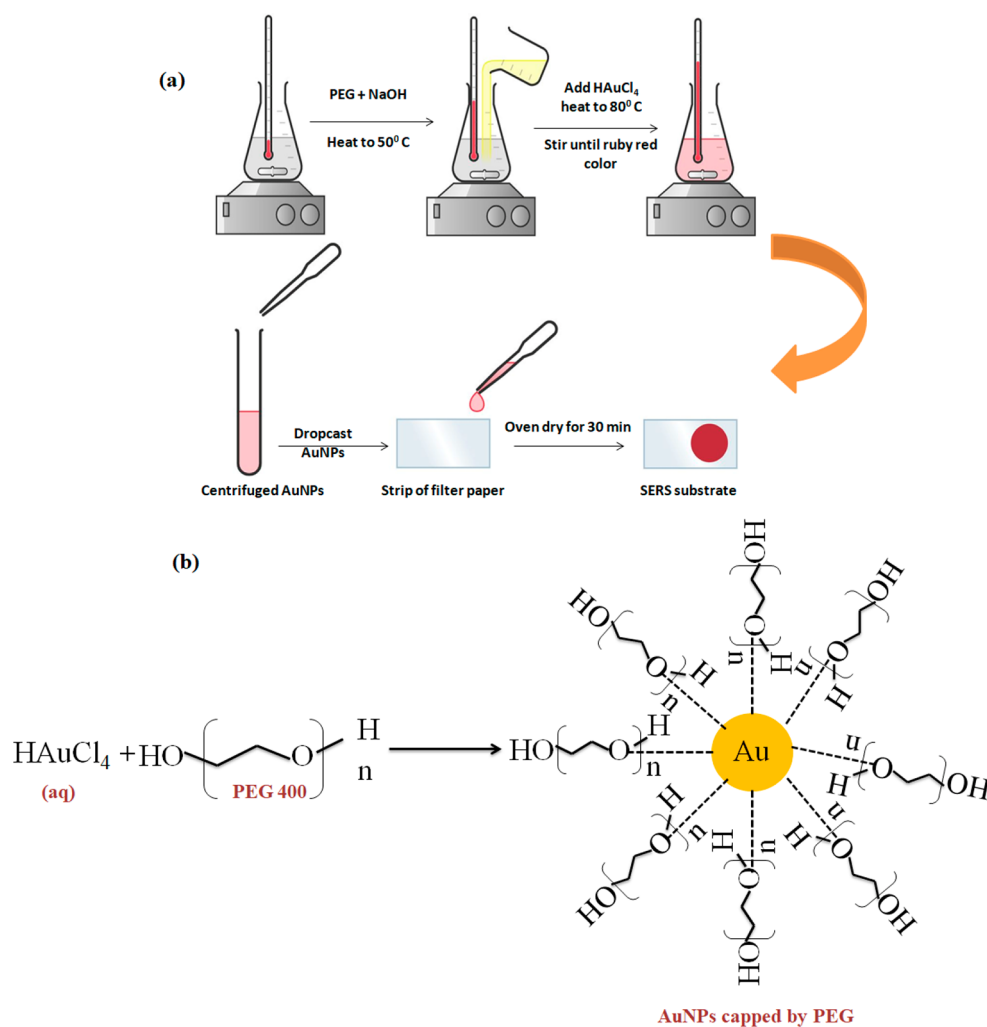


Figure 1. (a) Schematic illustration of the preparation of pegylated AuNPs and fabrication of the AuNPs hybrid SERS substrate. (b) Schematic illustration showing the interactions between the hydroxyl groups in PEG 400 present with the surface of AuNPs.

middle-income (LMICs) countries. Therefore, techniques such as SERS can be considered as a modern-day replacement for the techniques mentioned above in LMICs. SERS is fast, accurate, sensitive, and facile to use for the analysis of melamine in food.^{12–15}

SERS depends on the development of SERS-active substrates, and therefore, efforts continue to improve upon the SERS substrates. In recent years, advancement in SERS research has been constrained due to the complicated fabrication process of SERS substrates.¹⁶ The substrates are neither flexible, environmentally benign, nor economically viable. As a result, considerable effort has been put into creating high-performance and cost-effective SERS surfaces. In this regard, the advantages of paper-based flexible NPs hybrid SERS substrates are low cost and easy-to-design substrate.¹⁷ Additionally, flexible NPs hybrid SERS substrate shows high sensitivity and excellent reproducibility,^{18,19} thereby facilitating its use in food analysis, environmental safety, and forensic science.²⁰ When compared to smooth surface supports such as silicon wafers and metal film, special properties of paper, such as flexibility and hydrophilicity, are particularly well-suited for the analyses of samples with arbitrary shapes and levels. Additionally, the ridges on the paper's surface provide the formation of SERS hot spots.¹⁶ Numerous studies have been

done to hybridize plasmonic nanoparticles with paper using different techniques such as dip-coating, soaking, inkjet printing, screen printing, and vapor deposition of metal nanomaterials on the filter paper to create NPs hybrid SERS substrates. However, these techniques also have drawbacks. For example, dip-coating and soaking methods need comparatively more colloidal solution and prior research revealed that the soaking time was typically 1 to 2 days to achieve high SERS performance.²¹ This could result in the oxidation of NPs during the process as well as potential decay of the filter paper. In the case of inkjet printing, the use of high-viscosity dyes (NPs colloidal solution) for adequate loadings can lead to nozzle clogging at times.¹⁹ While the vapor-deposition method²² shows excellent reproducibility, it is not cost-effective and has difficult fabrication requirements. A new perspective is necessary to allow high-performance fast production of NPs hybrid paper-based SERS substrates.

A number of noble metal-based substrates, including Au, Ag, and Cu, have exceptional SERS capability for localized surface plasmon resonance (LSPR), generating hot spots, which is thought to be the primary method of achieving the SERS effect.²³ Much work has been put into creating efficient SERS substrates based on noble metals, metallic oxides (ZnO, SnO₂, TiO₂, and others), two-dimensional materials (graphene,

graphene oxide, and its derivatives, 2D Mxenes²⁴ as well as MoS₂), and metal–organic frameworks in the latest literature.²⁵ Silver and copper are among the major competitors that can be used as SERS substrates as these two show SERS enhancement that is comparable to the gold substrate but both silver and copper are more susceptible to oxidation and degradation, which can limit its long-term stability and hence can affect the reliability of the substrate. On the other hand, platinum and semiconductor materials are quite stable, but they do not show an enhancement factor that is comparable to that of gold due to weaker plasmonic properties. Therefore, among the noble metals mentioned above, gold is the chosen SERS substrate due to its strong plasmonic properties, chemical inertness, resistance to oxidation, and ease of synthesis.²³

Here, paper-based NPs hybrid substrates were constructed by drop-casting centrifuged pegylated AuNPs on filter paper. AuNPs were synthesized using poly(ethylene glycol) (PEG) 400 as a reducing agent via a facile and cost-effective method. The substrate was accessed for its application immediately after fabrication for qualitative and quantitative analysis of melamine. For quantitative analysis, Raman spectra of the melamine spiked sample were obtained and analyzed. The highest intensity Raman band at the wavelength(s) was considered the marker (control) band. The increase or decrease in the intensities of the marker band was observed in spiked samples at various concentrations. Calibration curves were plotted between the Raman intensities of the marker band against the logarithm of concentrations. The linear relation and high correlation coefficient (r) ≥ 0.99 were obtained to demonstrate the efficiency of substrate in quantitative analysis

2. MATERIALS AND INSTRUMENTS

Gold(III) chloride hydrate (HAuCl₄) was purchased from Sigma-Aldrich (St. Louis, MO, USA). PEG 400 and sodium hydroxide were obtained from Fisher Scientific (Mumbai, India). Rhodamine 6G (R6G) and melamine were obtained from CDH (Central Drug House, New Delhi, India). Whatman filter paper with a pore size of 11 μm and 125 mm diameter from Sigma-Aldrich (St. Louis, MO, USA) was used for substrate preparation. The size and morphology of AuNPs were characterized by UV–visible absorption spectroscopy (Tempstar double beam UV–visible spectrophotometer, India) and transmission electron microscopy (TEM; TEM-JEM-2100plus, JEOL Japan; 0.2 Å resolution). To check if the functional groups were present in the colloid suspension of AuNPs, Fourier transform infrared (FTIR) spectra of AuNPs were recorded on a Cary 630 FTIR (Agilent Technologies, New Delhi, India) between 400 and 4000 cm^{-1} . The RIAFMR-785-C (RI Nanotech, Uttarakhand, India) was used to capture Raman spectra at ambient temperatures (room temperature, that is, about 27 °C) with a 785 nm excitation monochromatic source. The same objective lens was used to collect the Raman scattered light in backscattering geometry, and a 1600 grooves/mm grating was employed as the dispersive element. For the observations, a 10 \times objective lens was used to focus the incident laser beam on the samples.

2.1. Synthesis of Pegylated Gold Nanoparticles (AuNPs) and Fabrication of NPs Hybrid SERS Substrate. The pegylated AuNPs were synthesized following the protocol as described by Stiufluoc et al. in 2013 with slight modifications.²⁶ Briefly, an initial solution (45 mL) containing

1.2 mL of 1% NaOH and 340 μL of PEG 400 was prepared in doubly distilled MilliQ water. This solution was placed on a programmable temperature controlled magnetic stirrer set to a temperature of 50 °C. A 5 mL aliquot of HAuCl₄ solution was rapidly added, and the reaction temperature was raised to 80 °C. This solution was stirred continuously until the solution turned ruby red (Figure 1a). The pegylated AuNPs produced by this method had a pH of 6.5. The colloidal suspension of pegylated AuNPs was centrifuged and washed three times. Furthermore, the bare sheets of filter paper were cut into strips of 1 cm \times 3 cm. Then, 5 μL of the centrifuged AuNPs was drop-cast on the filter paper strips and oven-dried at 50 °C for 30 min. The substrate produced in this way was ready for use immediately after drying. It can also be stored for several months and used if needed. The UV–vis spectra were used for AuNPs characterization.

2.2. Optimization of Nanoparticle Hybrid SERS Substrate and the Control. All SERS analyses in this article used the following methodology. A 10 μL amount of the test sample was applied to the paper-based flexible AuNPs hybrid SERS substrate in each experiment. The excitation laser wavelength was adjusted according to the analyte to be identified using SERS. Averaging over 10 scans, each spectrum was measured once with an accumulation duration of 1000 ms.

2.3. Powder Milk Sample Preparation for SERS Analysis. The powdered milk sample was created by mixing 500 mg of powdered milk with 100 mL of water. After that, a standard melamine solution was added to the milk sample to create a concentration gradient ranging between 10 and 0.01 ppm for SERS analysis. The SERS analysis was done using the method as described above (Section 2.2).

3. RESULTS AND DISCUSSION

3.1. Chemistry of Synthesis of Pegylated AuNPs. PEG 400 is a biopolymer, rich in the OH group and it is also affordable and adaptable.²⁷ Here, we present a straightforward, biocompatible, economical, and quick technique for synthesizing pegylated AuNPs using unmodified PEG, which serves as both a reducing and a stabilizing agent. AuNPs synthesized by other methods tend to self-assemble and agglomerate. Here, the OH group of PEG 400 acts as a reducing agent as well as a stabilizing agent and surrounds the AuNPs surface as shown in Figure 1b. This stabilization occurs due to van der Waals interactions between the OH of PEG 400 and AuNPs. The chain length of PEG 400 enhances the stabilization. In the process of experimenting in very mild circumstances, we observed, that the reduction of HAuCl₄ aqueous solution was significantly slow and made the formation of pegylated spherical AuNPs almost impossible in a very short time in the absence of alkaline media. Therefore, to make the HAuCl₄ aqueous solution, alkaline NaOH was added. As soon as NaOH solution was added to it, the pale-yellow color of the diluted HAuCl₄ aqueous solution changed to colorless. According to previous findings, this demonstrates the occurrence of a ligand-exchange reaction involving the tetrachloroaurate(III) ion.^{28,29} In general, the following process caused the tetrachloroaurate complex to have a couple of chloride ions substituted by hydroxide ions in the manner described as $[\text{AuCl}_4] + n\text{OH}^- \rightarrow [\text{AuCl}_{4-n}(\text{OH})_n] + n\text{Cl}^-$, a loss of the complex's yellow color, and a decrease in the extent of the ligand-to-metal charge transfer transition phenomenon, leading to a substantial blue shift in the absorption spectra.^{28,29} We can infer that the PEG 400 molecule oxidizes due to an

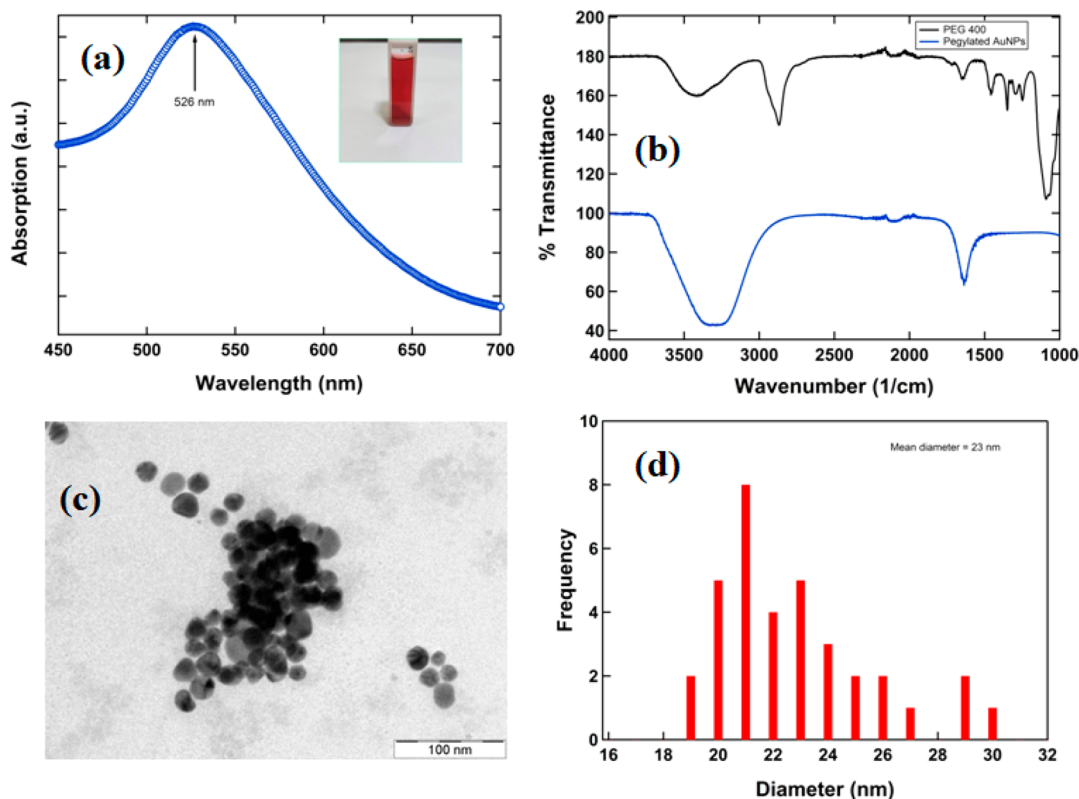


Figure 2. (a) UV–visible spectrum of AuNPs colloid with the picture of AuNPs colloidal solution in the inset. (b) FTIR spectra of PEG 400 and pegylated AuNPs. (c) TEM image of pegylated AuNPs. (d) Histogram of the size distribution of pegylated AuNPs.

alkaline reaction environment, even though hydroxy–gold(III) derivatives have higher reduction potentials than tetrachloroaurate(III) ions,³⁰ while the extra hydroxide ions facilitate the deprotonation of various reactions in the process with a subsequent shift in chemical equilibrium toward the formation of oxidation products.³¹ Therefore, NaOH and PEG 400 both play important roles in the preparation of pegylated AuNPs, where the former provides much-needed alkalinity to the solution and the latter causes the reduction of HAuCl₄ aqueous solution along with the stability of AuNPs.

3.2. Gold Nanoparticles (AuNPs) Characterization. The UV–visible spectrum of synthesized AuNPs exhibited a narrow and well-defined absorption band with an absorption maximum at ~526 nm, indicating a narrow size and shape of AuNPs³² particles (Figure 2a). From the UV–vis spectra, the average AuNPs particle size was estimated to be between 20 and 30 nm.^{33,26} To further confirm the particle size and morphology, AuNPs were characterized by TEM (transmission electron microscopy). The TEM image shown in Figure 2c suggests that most of the AuNPs were nearly spherical and polydisperse with a particle size of 20–25 nm. The average size from TEM was ~23 nm (Figure 2d).

FTIR is a technique used for the characterization of functional groups in compounds. The near-IR region (12500–4000 cm⁻¹) absorption provides information on the type of groups present in a molecule.³⁴ The data shown in Figure 2b depict the FTIR spectra of PEG 400 and pegylated AuNPs. The shift in the absorption bands in pegylated AuNPs confirms the synthesis of AuNPs due to PEG 400. The absorption bands at 3400, 2800, and 1100 cm⁻¹ in PEG 400 are due to OH stretching, –CH₂ stretching, and C–O stretching, respectively. The C–O peak has been shifted to

1300–1500 cm⁻¹ as AuNPs envelop it. The existence of a carbonyl group created through the oxidative transformation of PEG is indicated by an intense peak in a region of 1500–1700 cm⁻¹. The presence of an H-bonded O–H group in our sample is indicated by a broad peak in the wavenumber region 3300–3500 cm⁻¹.

3.3. SERS-Active Characterization and Enhancement Factor (EF) of AuNPs Hybrid Substrate. Due to the well-known vibrational characteristics of R6G, it was chosen as the sensor molecule to examine the SERS efficacy of the AuNPs hybrid substrate. Figure 3a shows Raman spectra of R6G at 10⁻⁵ M concentration with a AuNPs hybrid substrate and without the substrate. The Raman spectra of AuNPs hybrid substrate was also taken, and the results indicate that there is no contribution of the substrate in the SERS spectra of R6G. Figure 3b shows SERS spectra of varying concentrations (10⁻¹ to 10⁻⁸ M) of R6G when dropped onto the substrate and allowed to dry for 5 min before analysis. The most prominent Raman band at 1185 cm⁻¹ corresponds to C–H in-plane bending vibrations, whereas bands at 1363 and 1510 cm⁻¹ correspond to the aromatic C–C stretching vibrations.³⁵ The lowest concentration of 10⁻⁸ M also showed the prominent bands of R6G using this substrate, although the band intensity was significantly low.

With the help of spectral analysis of Figure 3b the SERS intensities centered at 1363 cm⁻¹ were plotted against the corresponding concentration, Figure 3c. This figure shows a smooth accent in values of SERS intensity with the increasing order of concentration of R6G. Thereafter a graph was plotted on logarithm-scale axes, between the log values of intensities (log *I*) and corresponding concentrations (log *C*), which was linear as shown in the inset of Figure 3c. This linear

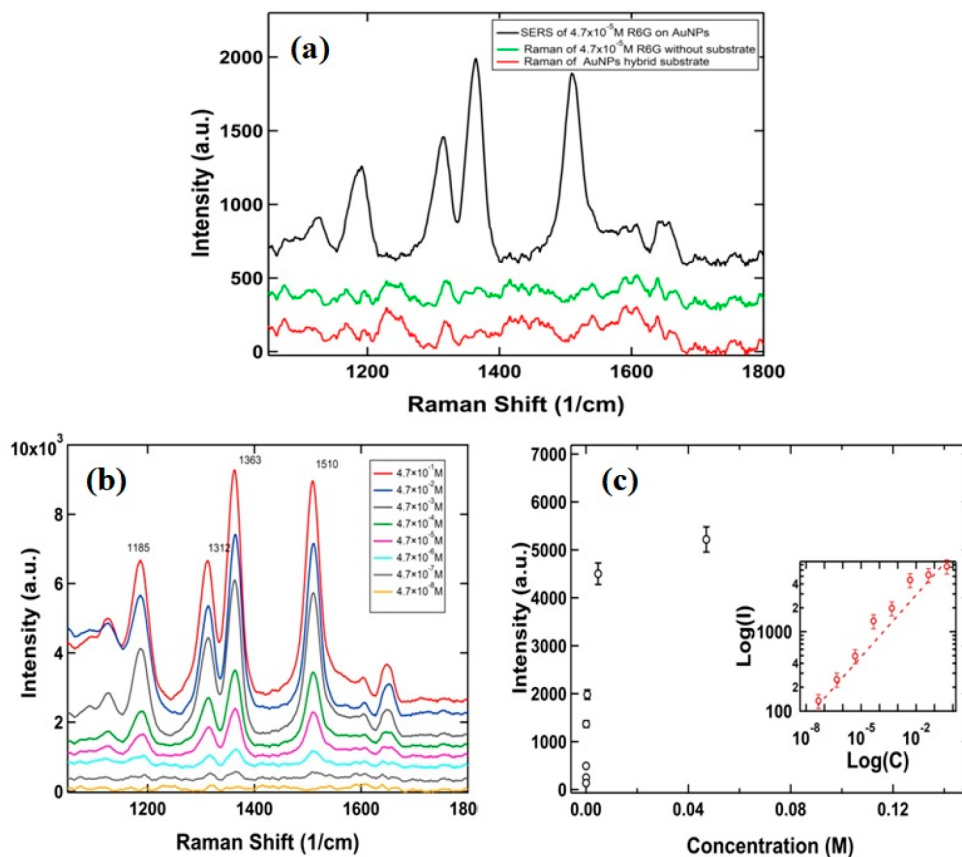


Figure 3. (a) Raman spectra of R6G at concentration 10^{-5} M with AuNPs hybrid substrate and without substrate and also Raman spectra of AuNPs hybrid substrate alone. (b) SERS spectra of R6G solutions of concentration ranging from 10^{-8} to 10^{-1} M. (c) Plot between the SERS intensity and corresponding concentration for the band centered at 1363 cm^{-1} . The inset shows the plot of log values of intensities ($\log I$) and corresponding concentrations ($\log C$).

relationship is discovered to be identical to earlier reports,³⁶ in which the Langmuir isotherm is followed to study the adsorption of analyte molecules.³⁵ As discussed in Section 1, this linear relationship can be utilized to calculate the unknown concentration of R6G using this substrate. To calculate the SERS enhancement factor (EF) of the paper-based flexible AuNPs hybrid substrate, the formula as shown in eq 1 was used:

$$EF = \left(\frac{I_{\text{SERS}}}{I_{\text{bare}}} \right) \left(\frac{C_{\text{bare}}}{C_{\text{SERS}}} \right) \quad (1)$$

where I_{SERS} and I_{bare} are the intensities of the SERS band and Raman band centered at 1363 cm^{-1} corresponding to concentrations $C_{\text{SERS}} = 4.7 \times 10^{-8}$ M and $C_{\text{bare}} = 4.5 \times 10^{-1}$ M, respectively.³⁵ Thus, the calculated EF for the prepared hybrid AuNPs substrate is on the order of 10^8 .

3.4. SERS Detection of Melamine in Solution. The frequent use of melamine as a cheap source of protein in dairy products calls for its efficient and fast detection. Here, the synthesized pegylated AuNPs hybrid substrate is utilized for the detection of melamine in dairy products. Figure 4a shows the Raman spectrum of pure melamine powder with sharp and clear bands at 587 , 677 , and 985 cm^{-1} . The bands at 677 and 985 cm^{-1} correspond to ring-breathing modes II and I of the triazine ring, respectively.³⁷ Thereafter a stock solution (1000 ppm) of melamine was created by stirring 100 mg of pure melamine powder into 100 mL of double-distilled water; this

stock solution was further diluted in water to create a series of melamine standard solutions with the following concentrations: 100 , 10 , 1 , 0.8 , 0.6 , 0.4 , 0.2 , 0.1 , and 0.01 ppm . The SERS spectra of solution concentrations of 100 , 10 , 1 , 0.4 , 0.1 , and 0.01 ppm are shown in Figure 4b. Here Raman bands that appear at 712 and 992 cm^{-1} in the SERS spectra show enhanced intensities for increased concentration of melamine. Along with the Raman spectrum of melamine solution of concentration 1000 ppm , a spectrum was also recorded of a sample in the absence of the hybrid substrate and none of the characteristic bands of melamine are visible in the spectrum, Figure 4b.

Here, surprisingly, Raman bands of melamine stock solution in SERS spectra exhibit a drastic shift from their actual position when they are associated with SERS substrate. This significant shift is of 35 and 7 cm^{-1} for the bands at 712 and 992 cm^{-1} , respectively, as compared to the bands in the Raman spectra of solid melamine.³⁸ In the quest to know the concentration where Raman bands start to shift for the sake of this SERS analysis of different concentrations between 1000 and 100 ppm , spectral analyses were also performed as shown in Figure 4c. It became obvious from the experiment that the shifting of both band positions 677 and 985 cm^{-1} started near about 600 ppm and followed the same trend in lower concentration thereafter. The shift in band position may be due to the effect of the enhancement mechanism.^{39,40} Thus, melamine detection via pegylated AuNPs hybrid substrates may become

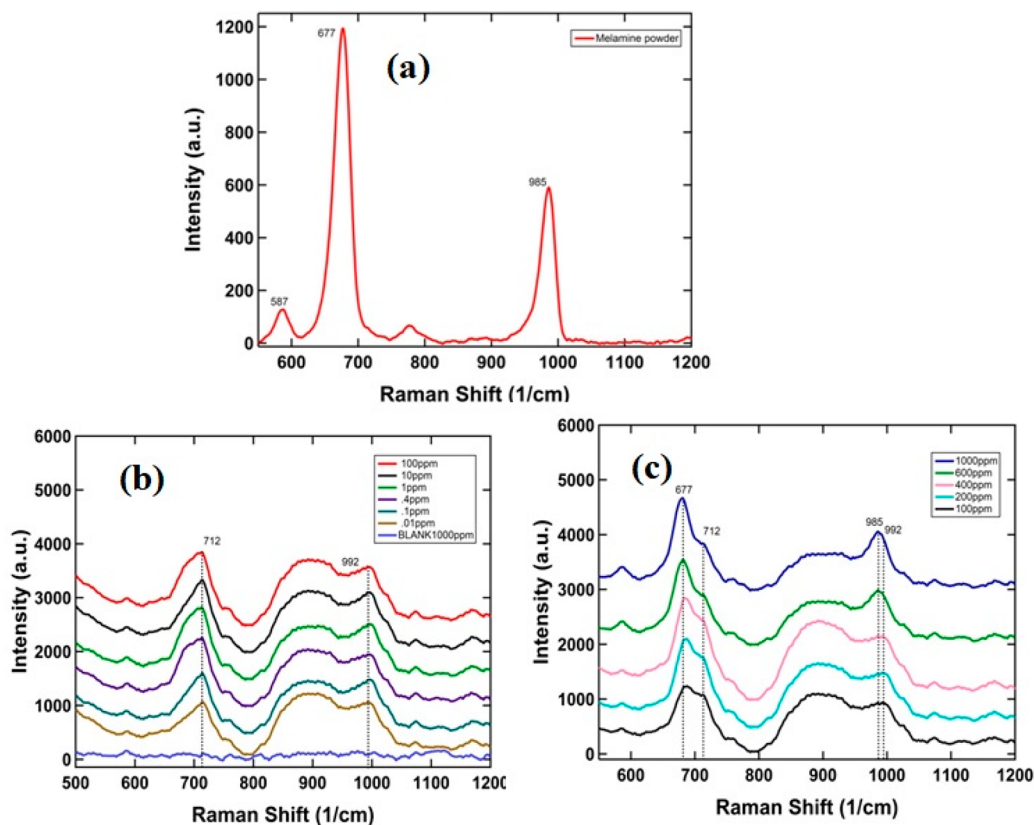


Figure 4. (a) Raman spectrum of powder melamine. (b) Raman spectra and SERS spectra of melamine for different concentrations. (c) Shift in SERS spectra peak as compared to different concentrations of solutions.

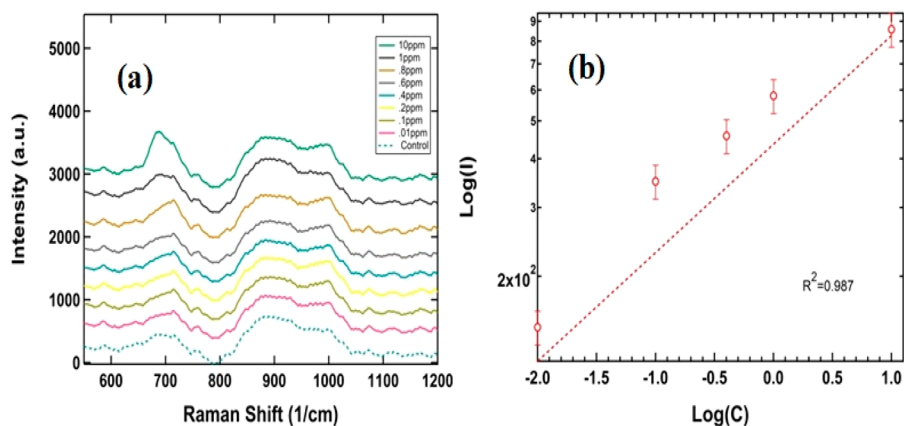


Figure 5. (a) SERS spectra of melamine spiked milk solution with a concentration ranging from 10 to 0.01 ppm. (b) Plot between the log values of intensities ($\log I$) and corresponding log values of concentrations ($\log C$) for the band centered at 712 cm^{-1} .

a promising tool to quantify melamine adulteration in various milk products.

3.5. Melamine Detection in a Spiked Milk Sample. In order to examine the selectivity of pegylated AuNPs hybrid substrate for melamine, this substrate was used to detect melamine in powder milk matrix.⁴¹ There are several different ingredients in milk, such as proteins, lipids, and carbs.⁴² A powder milk solution (100 mL) was spiked with 10 mg of melamine powder to create a concentration of 100 ppm of melamine in milk. From this concentration, 10, 1, 0.8, 0.6, 0.4, 0.2, 0.1, and 0.01 ppm melamine in milk were made through serial dilutions. Additionally, 1 mL of the spiked sample was put into a 1.5 mL centrifuge vial before being spun at 5000

rpm for 10 min. To quantify it, the supernatant was transferred to a clean vial for analysis. For reference, a milk sample devoid of melamine was used. Figure 5a shows SERS spectra of different concentrations (10, 1, 0.8, 0.6, 0.4, 0.2, 0.1, and 0.01 ppm) of melamine spiked milk samples. The bands at 712 and 992 cm^{-1} are distinctively visible, and the band intensity decreases as the concentration of melamine is reduced in the milk sample. Figure 5b shows an approximately straight line with a good determination coefficient ($R^2 \sim 0.987$) between the log values of intensities ($\log I$) and the corresponding log values of concentrations ($\log C$) for the band centered at 712 cm^{-1} . Table 1 summarizes the earlier reports related to the various substrates used for melamine detection that are

Table 1. SERS-Based Quantitative Detection of Melamine Using Different Nanoparticle-Based Substrates

S. no.	Nanoparticle-based substrate	Real food sample	LOD, ppm	Ref
1	Silver colloid	Liquid milk	0.5	12
2	Spherical magnetic-core gold-shell nanoparticles and rod-shaped gold nanoparticles labeled with 5,5'-dithiobis(2-nitrobenzoic acid)	Milk	0.39	13
3	Gold nanofinger SERS chips and the gel filtration method	Infant formula and whole milk	0.1	14
4	Gold nanoparticles	Liquid milk	0.17	39
5	Silver dendrite-based SERS substrate and immunological separation method	Milk	0.1	15
6	Gold nanospheres embedded monolith conjugates	Liquid milk	0.11	43
7	Silver nanoparticles	Milk	1	16
8	Ag nanoparticles deposited on a basil seed and then embedded into a small plastic box	Infant formula	0.11	44
9	Chitosan-modified silver nanoparticle paper	Whole milk	1	45
10	Silver film over nanospheres	Infant powder milk formula	2	46
11	Silver nanoparticles on the bio-scaffold arrays of cicada wings	Infant formula	10	35
12	Ag colloids	Milk	0.05	47
13	Silver nanodendrites (AgNDs) deposited onto a silicon surface	Liquid milk	0.10	7
14	Paper-based flexible AuNPs hybrid substrate	Powder milk	0.01	Current work

comparable to these results. The comparison with the previous reports indicates that AuNPs hybrid substrates used in the current research work involve a facile and cost-effective protocol. The LOD of melamine achieved in the current work is also low compared to other research reports.

4. CONCLUSION

In conclusion, a paper-based flexible AuNPs hybrid substrate, using Whatman filter paper of pore size 11 μm , was successfully prepared by drop-cast method to achieve a low-cost, uniform SERS substrate for the fast and accurate identification of melamine in powder milk. The pegylated AuNPs utilized here were spherical with an average particle size of ~ 23 nm. FTIR analysis confirmed the protective layer of PEG on AuNPs, thereby providing much-needed stability. SERS characterization of the substrate using R6G exhibited desirable signal sensitivity, reproducibility, enhancement factor (10^8), and appreciably low LOD (10^{-8} M). Further, to demonstrate the practical applicability of the AuNPs hybrid SERS substrate in real world samples, it was utilized to detect the melamine in spiked milk samples and showed a melamine characteristic band for the concentration as low as 0.01 ppm. Thus, it is a desirable substrate for application in food analysis.

AUTHOR INFORMATION

Corresponding Author

Anil K. Yadav – Department of Physics, Chaudhary Charan Singh University, Meerut 250004, India; orcid.org/0000-0003-1160-0012; Email: anilphy@ccsuniversity.ac.in

Authors

Akanksha Yadav – Department of Physics, Chaudhary Charan Singh University, Meerut 250004, India

Nazia Tarannum – Department of Chemistry, Chaudhary Charan Singh University, Meerut 250004, India

Dev Kumar – Department of Physics, Chaudhary Charan Singh University, Meerut 250004, India

Complete contact information is available at: <https://pubs.acs.org/10.1021/acsomega.3c07663>

Notes

The authors declare no competing financial interest.

ACKNOWLEDGMENTS

The A.K.Y. is grateful for financial support for creating this work from the scheme grant and aid of the Department of Health Research (DHR), Indian Council of Medical Research (ICMR), India (P. No. R.11012/04/2019-HR). Authors are also grateful for partial financial support provided by Ch. Charan Singh University, Meerut, under the University Research Grant Scheme (URGS) project (Ref. No. Dev/URGS/2022-23/36).

REFERENCES

- Albrecht, M. G.; Creighton, J. A. Anomalous intense Raman spectra of pyridine at a silver electrode. *J. Am. Chem. Soc.* **1977**, *99* (15), 5215–5217.
- Zhang, D.; Pu, H.; Huang, L.; Sun, D. W. Advances in flexible surface-enhanced Raman scattering (SERS) substrates for non-destructive food detection: Fundamentals and recent applications. *Trends in Food Science & Technology* **2021**, *109*, 690–701.
- Cang, H.; Labno, A.; Lu, C.; Yin, X.; Liu, M.; Gladden, C.; Liu, Y.; Zhang, X. Probing the electromagnetic field of a 15-nanometre hotspot by single molecule imaging. *Nature* **2011**, *469* (7330), 385–388.
- Cavin, C.; Cottenet, G.; Fuerer, C.; Tran, L. A.; Zbinden, P. Food fraud vulnerabilities in the supply chain: an industry perspective. In *Encyclopedia of Food Chemistry*; Elsevier, 2019; Vol. 1, pp 670–678. DOI: [10.1016/B978-0-08-100596-5.21788-5](https://doi.org/10.1016/B978-0-08-100596-5.21788-5).
- Food Safety and Standards Authority of India (FSSAI). *Annual report 2018–2019*; FSSAI, 2019; p 131.
- Burns, K.; Nolen, S.; Kahler, S.; Rezendes, A. Recall of pet food leaves veterinarians seeking solutions. *J. Am. Vet. Med. Assoc.* **2007**, *230* (8), 1128–1129.
- Cuong, N. M.; Cao, D. T.; Thu, V. T.; Ngan, L. T.-Q. Direct detection of melamine in liquid milk and infant formula using surface-enhanced Raman scattering combined with silver nanodendrites. *Optik* **2021**, *243*, 167504.
- Sivashanmugan, K.; Liao, J. D.; Liu, B. H.; Yao, C. K. Focused-beam-fabricated Au nanorods coupled with Ag nanoparticles used as surface-enhanced Raman scattering-active substrate for analyzing trace melamine constituents in solution. *Analytica chimica acta* **2013**, *800*, 56–64.

- (9) Chan, E. Y. Y.; Griffiths, S. M.; Chan, C. W. Public-health risks of melamine in milk products. *Lancet* **2008**, 372 (9648), 1444–1445.
- (10) Squadrone, S.; Ferro, G. L.; Marchis, D.; Mauro, C.; Palmegiano, P.; Amato, G.; et al. Determination of melamine in feed: Validation of a gas chromatography-mass spectrometry method according to 2004/882/CE regulation. *Food Control* **2010**, 21 (5), 714–718.
- (11) Tyan, Y.-C.; Yang, M.-H.; Jong, S.-B.; Wang, C.-K.; Shiea, J. Melamine contamination. *Anal. Bioanal. Chem.* **2009**, 395 (3), 729–735.
- (12) Zhang, X. F.; Zou, M. Q.; Qi, X. H.; Liu, F.; Zhu, X. H.; Zhao, B. H. Detection of melamine in liquid milk using surface-enhanced Raman scattering spectroscopy. *J. Raman Spectrosc.* **2010**, 41 (12), 1655–1660.
- (13) Yazgan, N. N.; Boyaci, İ. H.; Topcu, A.; Tamer, U. Detection of melamine in milk by surface-enhanced Raman spectroscopy coupled with magnetic and Raman-labeled nanoparticles. *Anal. Bioanal. Chem.* **2012**, 403, 2009–2017.
- (14) Kim, A.; Barcelo, S. J.; Williams, R. S.; Li, Z. Melamine sensing in milk products by using surface enhanced Raman scattering. *Analytical chemistry* **2012**, 84 (21), 9303–9309.
- (15) Li, X.; Feng, S.; Hu, Y.; Sheng, W.; Zhang, Y.; Yuan, S.; Zeng, H.; Wang, S.; Lu, X. Rapid detection of melamine in milk using immunological separation and surface enhanced Raman spectroscopy. *J. Food Sci.* **2015**, 80 (6), C1196–C1201.
- (16) Zhang, C.; You, T.; Yang, N.; Gao, Y.; Jiang, L.; Yin, P. Hydrophobic paper-based SERS platform for direct-droplet quantitative determination of melamine. *Food chemistry* **2019**, 287, 363–368.
- (17) Betz, J. F.; Yu, W. W.; Cheng, Y.; White, I. M.; Rubloff, G. W. Simple SERS substrates: powerful, portable, and full of potential. *Phys. Chem. Chem. Phys.* **2014**, 16 (6), 2224–2239.
- (18) Ngo, Y. H.; Li, D.; Simon, G. P.; Garnier, G. Gold nanoparticle-paper as a three-dimensional surface enhanced Raman scattering substrate. *Langmuir* **2012**, 28 (23), 8782–8790.
- (19) Hoppmann, E. P.; Wei, W. Y.; White, I. M. Inkjet-printed fluidic paper devices for chemical and biological analytics using surface enhanced Raman spectroscopy. *IEEE J. Select. Top. Quantum Electron.* **2014**, 20 (3), 195–204.
- (20) Fierro-Mercado, P. M.; Hernández-Rivera, S. P. Highly sensitive filter paper substrate for SERS trace explosives detection. *Int. J. Spectrosc.* **2012**, 2012, 716527.
- (21) Lee, C. H.; Tian, L.; Singamaneni, S. Paper-based SERS swab for rapid trace detection on real-world surfaces. *ACS Appl. Mater. Interfaces* **2010**, 2 (12), 3429–3435.
- (22) Gupta, R.; Weimer, W. A. High enhancement factor gold films for surface enhanced Raman spectroscopy. *Chemical physics letters* **2003**, 374 (3–4), 302–306.
- (23) Zhang, C.; Jiang, S. Z.; Huo, Y. Y.; Liu, A. H.; Xu, S. C.; Liu, X. Y.; Sun, Z. C.; Xu, Y. Y.; Li, Z.; Man, B. Y. SERS detection of R6G based on a novel graphene oxide/silver nanoparticles/silicon pyramid arrays structure. *Opt. Express* **2015**, 23 (19), 24811–24821.
- (24) Tyagi, N.; Sharma, G.; Kumar, D.; Pratap Neelratan, P.; Sharma, D.; Khanuja, M.; Singh, M. K.; Singh, V.; Kaushik, A.; Sharma, S. K. 2D-MXenes to tackle wastewater: From purification to SERS-based sensing. *Coord. Chem. Rev.* **2023**, 496, 215394.
- (25) Gushiken, N. K.; Paganoto, G. T.; Temperini, M. L.; Teixeira, F. S.; Salvadori, M. C. Substrate for surface-enhanced Raman spectroscopy formed by gold nanoparticles buried in poly (methyl methacrylate). *ACS omega* **2020**, 5 (18), 10366–10373.
- (26) Stiuflu, R.; Iacovita, C.; Nicoara, R.; Stiuflu, G.; Florea, A.; Achim, M.; Lucaciu, C. M. One-step synthesis of PEGylated gold nanoparticles with tunable surface charge. *J. Nanomater.* **2013**, 2013, 146031.
- (27) Jokerst, J. V.; Lobovkina, T.; Zare, R. N.; Gambhir, S. S. Nanoparticle PEGylation for imaging and therapy. *Nanomedicine* **2011**, 6 (4), 715–728.
- (28) Ojea-Jiménez, I.; Campanera, J. M. Molecular modeling of the reduction mechanism in the citrate-mediated synthesis of gold nanoparticles. *J. Phys. Chem. C* **2012**, 116 (44), 23682–23691.
- (29) Farges, F.; Sharps, J. A.; Brown, G. E., Jr. Local environment around gold (III) in aqueous chloride solutions: An EXAFS spectroscopy study. *Geochim. Cosmochim. Acta* **1993**, 57 (6), 1243–1252.
- (30) Vanysek, P. Electrochemical series. *CRC Handbook of Chemistry and Physics*, Vol. 8; Taylor & Francis Group, 1999.
- (31) Nitica, S.; Moldovan, A. I.; Toma, V.; Moldovan, C. S.; Berindan-Neagoe, I.; Stiuflu, G.; Lucaciu, C. M.; Stiuflu, R. PEGylated gold nanoparticles with interesting plasmonic properties synthesized using an original, rapid, and easy-to-implement procedure. *J. Nanomater.* **2018**, 2018, 5954028.
- (32) Bohren, C. F.; Huffman, D. R. *Absorption and scattering of light by small particles*; John Wiley & Sons, 2008.
- (33) Borse, V.; Konwar, A. N. Synthesis and characterization of gold nanoparticles as a sensing tool for the lateral flow immunoassay development. *Sensors International* **2020**, 1, 100051.
- (34) Manson, J.; Kumar, D.; Meenan, B. J.; Dixon, D. Polyethylene glycol functionalized gold nanoparticles: the influence of capping density on stability in various media. *Gold bulletin* **2011**, 44, 99–105.
- (35) Zhao, N.; Li, H.; Tian, C.; Xie, Y.; Feng, Z.; Wang, Z.; Yan, X.; Wang, W.; Yu, H. Bioscaffold arrays decorated with Ag nanoparticles as a SERS substrate for direct detection of melamine in infant formula. *RSC Adv.* **2019**, 9 (38), 21771–21776.
- (36) Wu, W.; Hu, M.; Ou, F. S.; Williams, R. S.; Li, Z. Rational engineering of highly sensitive SERS substrate based on nanocone structures. In *Advanced Environmental, Chemical, and Biological Sensing Technologies VII*, Vol. 7673; 2010; pp 161–166. SPIE. DOI: 10.1117/12.849959.
- (37) Koglin, E.; Kip, B. J.; Meier, R. J. Adsorption and displacement of melamine at the Ag/electrolyte interface probed by surface-enhanced Raman microprobe spectroscopy. *J. Phys. Chem.* **1996**, 100 (12), 5078–5089.
- (38) Giovannozzi, A. M.; Rolle, F.; Sega, M.; Abete, M. C.; Marchis, D.; Rossi, A. M. Rapid and sensitive detection of melamine in milk with gold nanoparticles by Surface Enhanced Raman Scattering. *Food chemistry* **2014**, 159, 250–256.
- (39) Haynes, C. L.; McFarland, A. D.; Van Duyne, R. P. Surface-enhanced Raman spectroscopy. *Anal. Chem.* **2005**, 77, 338A–346A.
- (40) He, L.; Liu, Y.; Lin, M.; Awika, J.; Ledoux, D. R.; Li, H.; Mustapha, A. A new approach to measure melamine, cyanuric acid, and melamine cyanurate using surface enhanced Raman spectroscopy coupled with gold nanosubstrates. *Sensing and Instrumentation for Food Quality and Safety* **2008**, 2, 66–71.
- (41) Mecker, L. C.; Tyner, K. M.; Kauffman, J. F.; Arzhantsev, S.; Mans, D. J.; Gryniwicz-Ruzicka, C. M. Selective melamine detection in multiple sample matrices with a portable Raman instrument using surface enhanced Raman spectroscopy-active gold nanoparticles. *Analytica chimica acta* **2012**, 733, 48–55.
- (42) Xiong, Z.; Chen, X.; Liou, P.; Lin, M. Development of nanofibrillated cellulose coated with gold nanoparticles for measurement of melamine by SERS. *Cellulose* **2017**, 24, 2801–2811.
- (43) Kaleem, A.; Azmat, M.; Sharma, A.; Shen, G.; Ding, X. Melamine detection in liquid milk based on selective porous polymer monolith mediated with gold nanospheres by using surface enhanced Raman scattering. *Food chemistry* **2019**, 277, 624–631.
- (44) Zhou, N.; Zhou, Q.; Meng, G.; Huang, Z.; Ke, Y.; Liu, J.; Wu, N. Incorporation of a basil-seed-based surface enhanced Raman scattering sensor with a pipet for detection of melamine. *ACS Sensors* **2016**, 1 (10), 1193–1197.
- (45) Li, D.; Lv, D. Y.; Zhu, Q. X.; Li, H.; Chen, H.; Wu, M. M.; Chai, Y. F.; Lu, F. Chromatographic separation and detection of contaminants from whole milk powder using a chitosan-modified silver nanoparticles surface-enhanced Raman scattering device. *Food chemistry* **2017**, 224, 382–389.
- (46) Xiao, G.; Li, L.; Yan, A.; He, X. Direct detection of melamine in infant formula milk powder solution based on SERS effect of silver film over nanospheres. *Spectrochimica Acta Part A: Molecular and Biomolecular Spectroscopy* **2019**, 223, 117269.

(47) Liu, S.; Kannegulla, A.; Kong, X.; Sun, R.; Liu, Y.; Wang, R.; Yu, Q.; Wang, A. X. Simultaneous colorimetric and surface-enhanced Raman scattering detection of melamine from milk. *Spectrochim. Acta, Part A* **2020**, *231*, 118130.